International Journal of Thin Films Science and Technology

http://dx.doi.org/10.18576/ijtfst/130310

Heat Flow in Magnetohydrodynamics Micropolar Casson Fluid with Thermal Radiation Due to Stretching Sheet

Ajay Nandan[1], *Bhupander Singh*[1], *Mahmoud Abdel-Aty*[2,3], *and Kottakkaran Sooppy Nisar*[4]*

[1]Department of Mathematics, Meerut College, Meerut (UP), India
[2]Deanship of Graduate Studies and Research, Ahlia University, P.O. Box 10878 Manama, Kingdom of Bahrain
[3]Jadara Research Center, Jadara University, P.O. Box 733, Irbid, 21110, Jordan
[4]Department of Mathematics, College of Science and Humanities in Alkharj, Prince Sattam Bin Abdulaziz University, Alkharj, 11942, Saudi Arabia

Received: 10 Jun 2024, Revised: 11 Aug. 2024, Accepted: 21 Aug. 2024
Published online: 1 Sep. 2024

Abstract: A theoretical inspection of transfer of heat in magnetohydrodynamic micropolar Casson fluid influence of stretching sheet in porous media with thermal radiation is worked out. The governing nonlinear partial differential equations of the problem after similarity transformations are used to turn them into a system of ordinary differential equations which are solved numerically via Differential Transformation Method (DTM). The DTM solution is explored by bvp4c numerical solver built in MATLAB. The effect of several variables(parameters) on velocity profile, distribution of temperature and microrotation are explained with graphs.

Keywords: Magnetohydrodynamics, Heat Transfer, Casson Fluid, Thermal Radiation, Porous Medium.

1 Introduction

Wide-ranging applications of micropolar theory can be found in many branches of research and engineering. For the first time, Eringen introduced the micropolar fluid theory in [1,2]. Willson [3], Kilne [4], Adan [5], Gorla [6] analyzed the flows along horizontal and vertical planes. Applications of flow and transfer of heat of viscous fluid(incompressible) across a stretching sheet are significant in many fields viz. polymer's extrusion, heating down metallic plates, plastic sheet's aerodynamic extrusion, etc. such processes are needed to analyze the quality of the end products. Crane [7] studied the flow of an ambient fluid across a stretching sheet (linearly) and gave a correspondence solution for the two-dimensional problem's steady in the form of closed analytical.

Ariman et al. [8] studied the applications of micropolar and thermo-micropolar fluids in engineering and technology. Prathap Kumar et al. [9] examined micropolar viscous fluid for fully convective flow via vertical channel. Effect of surface conditions analyzed by Kelson and Desseaux [10] guided by a porous sheet that has to be stretched on the micropolar flow. The unsteady flow between two parallel micropolar fluid porous plates analyzed by Srinivasacharya et al. [11]. Bhargava et al. [12] has illustrated the mixed convection flow with micropolar fluid inclusion of consistent suction via porous sheet with the help of numerical technique i.e. Finite Element Method (FEM). Ibrahim et al. [13] illustrated the micropolar fluid's mixed convection flow situation travelling through a semi-infinite porous plate while experiencing viscous dissipation and thermal radiation with changing suction velocity normal to the plate.

Ali and Magyari [14] discussed the fluid's erratic movement along with the heat transfer by a submerged stretched surface was explored with numerical solutions. Mukhopadhyay [15] expanded on the work of Ali and Magyari [14] by supposing that thermal diffusivity and viscosity are of temperature's linear functions and then discussed the boundary layer flow(BLF) of an unsteady mix convection of viscous fluid(incompressible) along a permeable surface through a porous media, as well as the thermal radiation impact on heat transfer. The melting heat flow for a micropolar fluid in BLF because of stagnation point flow towards a shrinking/stretching sheet was studied, with reference to the work of Yacos et al. [16]. Rosali et al. [17] developed the theory of micropolar fluid in a porous media towards a contracting /stretching sheet with suction analysis. They solved their system of governing equations numerically. Bhukta et al. [18] developed

* Corresponding author e-mail: n.sooppy@psau.edu.sa

the Magneto hydrodynamic flow across a contracting sheet in porous media and was discussed in detail in their study. The heat transfer MHD flow across a surface that has been stretched, including the heat generation slip velocity and absorption effect of a micropolar fluid has been studied by Mahmood and Waheed [19]. Shahzad, et al. [20] discussed thermal radiation's impact on magnetohydrodynamic flow at an axisymmetric stagnation point and impact of heat exchange for a micropolar fluid on top of a contracting sheet. Eldabe, et al. [21] examined Sherwood number and Nusselt number impacts of physical parameters on MHD peristaltic flow with mass and heat transfer of micropolar bi-viscosity fluid between two co-axial tubes via a porous material.

There are several practical applications of streaming through a porous material particularly in geo- physical fluid dynamics. Some examples of naturally porous media include sandstone, beach sand, limestone, the human lung, and the gall bladder of tiny blood veins with stones. Eldabe, et al. [22] studied pulsatile flow's impact on heat and mass transport in MHD with couple stress for Casson fluid through porous medium. Mekheimer [23] stated the non-linear peristaltic transport in a planar channel which was inclined across a porous medium. The mixed convection Magnetohydrodynamics flow with the collective transfer of mass and heat with chemical reaction along a porous plate in existence of heat source studied by Zueco and Ahmed [24] and they observe that the fluid temperature, the flow velocity when the destructive chemical process is accelerated, the magnetic field is produced decreases. One of the important uses of Casson fluid model is to forecast the flow of blood at low down shear rate in arteries. Also, it is utilized in perception flow conduct of printing ink pigment oil suspensions. Mehmoo et al. [25] numerically investigated the micropolar Casson fluid with internal heating across a sheet(stretching). Iqbal et al. [26] used the Keller box technique to investigate the effect of IMF (inclined magnetic field) on micropolar Casson fluid. To fill the literature gap discussed above, we formulated the above problem and discussed the outcomes so obtained.

2 Mathematical formulation

We assumed a two-dimensional flow of an incompressible magnetohydrodynamic micropolar Casson fluid in a porous material, with heat radiation occurring across a stretched sheet. The X-axis corresponds to the motion direction with respect to the surface of the sheet that is being stretched or shrunk, while the Y-axis is perpendicular to that surface. Suppose the surface of stretching sheet has the velocity $u = u_w = ax$, where a is a real constant. For an incompressible flow the Casson fluid's state rheological

$$\tau_{ij} = \begin{cases} 2(\mu_B + \frac{p_y}{\sqrt{2\pi}})e_{ij}, \pi > \pi_c, \\ 2(\mu_B + \frac{p_y}{\sqrt{2\pi}})e_{ij}, \pi < \pi_c \end{cases}$$

The product of the deformation rate component, where the component $(i, j)^{th}$ of e_{ij} represents the rate of deformation $\pi = e_{ij}e_{ij}$, μ_B is the non-Newtonian fluid's plastic dynamic viscosity , p_y yields fluid stress. The guiding equations are as

$$\frac{\partial u}{\partial x} + \frac{\partial v}{\partial v} = 0 \tag{1}$$

$$u\frac{\partial u}{\partial x} + v\frac{\partial v}{\partial v} = \nu(1 + \frac{k}{\mu} + \frac{1}{\beta})\frac{\partial^2 u}{\partial y^2} - \frac{\sigma B_0^2 u}{\rho} + \frac{k}{\rho}\frac{\partial N}{\partial y} - \frac{\mu}{\rho k_1}u \tag{2}$$

$$u\frac{\partial T}{\partial x} + v\frac{\partial T}{\partial v} = \frac{k}{\rho c_p}\frac{\partial^2 T}{\partial y^2} - \frac{1}{\rho c_p} + \frac{k}{\rho}\frac{\partial q_r}{\partial y} + \frac{\mu}{\rho c_p}(\frac{\partial u}{\partial y})^2 \tag{3}$$

$$u\frac{\partial N}{\partial x} + v\frac{\partial N}{\partial y} = \frac{\gamma}{\rho_j}\frac{\partial^2 N}{\partial y^2} - \frac{k}{\rho_j}(2N + \frac{\partial u}{\partial y}) \tag{4}$$

With the problem's proper conditions of boundary are provided by

$$u = u_w = ax, \quad v = 0, \quad N = -n\frac{\partial u}{\partial y}, \quad T = T_w \quad \text{at} \quad y = 0 \tag{5a}$$

$$u \to 0, \quad N \to 0, \quad T \to T_\infty \quad \text{at} \quad y \to \infty, \tag{5b}$$

here u and v are the X- and Y-axis velocities; β is the Casson Fluid Parameter; N is the micro- or angular rotation velocity; P is the fluid pressure; ρ is the fluid density; c_p is the specific heat at constant pressure; k is the thermal conductivity;

j is the micro-inertia density and T is the fluid temperature. The n is the fluid's boundary concentration parameter, the case $n = 0$ and $n = 0.5$ are represent strong concentration and weak concentrations, respectively. Now, under Rosseland diffusion approximation the thermal radiation is simulated and in due account of the q_r defined as follows:

$$q_r = -\frac{4\sigma^*}{3\sigma k^*}\frac{\partial T^4}{\partial y} \tag{6a}$$

$$\frac{\partial q_r}{\partial y} = -\frac{16\sigma^* T_\infty^3}{3\sigma k^*}\frac{\partial^2 T}{\partial y^2}, \tag{6b}$$

In this case, the Stefan-Boltzmann constant is σ^*, and k^* is the Rosseland mean absorption coefficient. We are expanding T^4 by using Taylor's series about T_∞. Therefore, we gain the $T^4 = 4T_\infty^3 T - 3T_\infty^4$ (when temperature difference is sufficiently small). The following Similarities variables are now introduced:

$$u = ax\frac{\partial f}{\partial \eta}, \quad \eta = \sqrt{\frac{a}{\nu}}y, \quad v = -\sqrt{a\nu}f(\eta), \quad N = a\sqrt{\frac{a}{\nu}}xg(\eta), \quad \theta(\eta) = \frac{T - T_\infty}{T_w - T_\infty} \tag{7}$$

By using equations (5a) – (7), equations (2) – (4) transformed into the equations

$$(1 + A + \frac{1}{\beta})f'''(\eta) + f(\eta)f''(\eta) - (f'(\eta))^2 - (M + K_P)f'(\eta) + Ag'(\eta) = 0 \tag{8}$$

$$(1 + \frac{4}{3R})\theta''(\eta) + P_r f(\eta)\theta'(\eta) + P_r E_c (f''(\eta))^2 = 0 \tag{9}$$

$$(1 + \frac{A}{2})g''(\eta) + f(\eta)g'(\eta) - f'(\eta)g(\eta) - A(2g(\eta) + f''(\eta)) = 0 \tag{10}$$

Boundary conditions (5a) and (5b) in similarity variables become

$$f(0) = 0, \quad f'(0) = 0, g(0) = -nf''(0), \quad \theta(0) = 1 \tag{11a}$$

$$f'(\eta) \to 0, \quad g(\eta) \to \infty, \quad \theta(\eta) \to \infty(0), \quad \text{as} \quad n \to \infty, \tag{11b}$$

Where $A = k/\mu$, (Micropolar Parameter), $M = (\sigma B_0^2)/\rho a$, (Magnetic Parameter) $K_p = \mu/(\rho a k_1)$, (Porosity Parameter), $P_r = (\mu C_P)/\kappa$, (Prandtl Number) $R = (4\sigma^* T_\infty^3)/(3\kappa K^*)$, (Radiation Parameter), $E_c = (a^2x^2)/(C_P(T_w - T_\infty))$, (Eckert Number)

3 Method of solution

Fundamentals of DTM (differential transformation method) [27] are explored as given below: Differential transformation of the k^{th}derivative of a function $f(\eta)$ is defined as

$$F(k) = \frac{1}{k!}\left[\frac{d^k f(\eta)}{d\eta^k}\right]_{\eta=\eta_0} \tag{12}$$

Where $(\mathbf{k})$ is called the T function of $f(\eta)$ at $\eta = \eta_0$ in $\mathbf{k}-$domain. Defining inverse transformation of $(\mathbf{k})$ as

$$f(\eta) = \sum_{k=0}^{\infty} F(k)(\eta - \eta_0)^k \tag{13}$$

From Eqs (12) and (13), $f(\eta)$ can be obtained as

$$f(\eta) = \sum_{k=0}^{\infty} \frac{1}{k!}\left[\frac{d^k f(\eta)}{d\eta^k}\right]_{\eta=\eta_0} (\eta - \eta_0)^k \tag{14}$$

In practice, to achieve a finite one, this infinite series truncated as follows

$$f(\eta) = \sum_{k=0}^{N} F(k)(\eta - \eta_0)^k \tag{15}$$

Equations (12)-(13) can be used to determine theorems to be employed in the transformation process, which are given in table 1.

Table 1: Table of conversions

Primary Function	Function that has been transformed
$f(\eta)=\alpha g(\eta)\pm\beta h(\eta)$	$F[k]=\alpha G[k]+\beta H[k]$
$f(\eta)=\frac{d^n f(\eta)}{df(\eta)}$	$F[k]=\frac{(k+\eta)!}{k!}G[(k+\eta)]$
$f(\eta)=g(\eta)h(\eta)$	$F(k)=\sum_{m=0}kF(m)H(k-m)$
$f(\eta)=e^{m\eta}$	$F(k)=\frac{m^k}{k!}$
$f(\eta)=(\eta)^m$	$F(k)=\delta(k-m)=\begin{cases}1,k=m\\0,k\neq m\end{cases}$
$f(\eta)=(1+\eta)^m$	$F(k)=\frac{(m)(m-1)...(m-k+1)}{k!}$
$f(\eta)=\sin(\omega\eta+\alpha)$	$F(k)=\frac{\omega^k}{k!}\sin(\frac{\pi k}{2}+\alpha)$
$f(\eta)=\cos(\omega\eta+\alpha)$	$F(k)=\frac{\omega^k}{k!}\cos(\frac{\pi k}{2}+\alpha)$

4 DTM Solution of the problem

Applying differential transformation method to (7) - (9), we obtain

$$\left(1+A+\frac{1}{\beta}\right)(K+1)(K+2)(K+3)F[K+3]+\left[\sum_{m=0}^{K}F[K-m](m+1)(m+2)F[m+2]\right]$$
$$-\left[\sum_{m=0}^{K}(K-m+1)F[K-m+1](m+1)F[m+1]\right]-(M+K_p)(K+1)F(K+1)+A(K+1)G(K+1)=0 \tag{16}$$

$$(1+\frac{4}{3}R)(K+1)(K+2)\theta[K+2]+P_r\left[\sum_{m=0}^{K}F[K-m].(m+1)\theta[m+1]\right]$$
$$+P_rE_c\left[\sum_{m=0}^{K}(K-m+2)(K-m+1)F[K-m+2].(m+1)(m+2)F[m+2]\right]=0 \tag{17}$$

$$(1+\frac{A}{2})(K+1)(K+2)G[K+2]+\left[\sum_{m=0}^{K}F[K-m].(m+1)G[m+1]\right]$$
$$-\left[\sum_{m=0}^{K}G[K-m].(m+1)F[m+1]\right]-A[2G[K]+(K+1)(K+2)F(K+2)]=0 \tag{18}$$

With governing conditions

$$F[0]=0,\qquad F[1]=1,\qquad F[2]=\alpha_1$$
$$G[0]=-2n\alpha_1,\qquad G[1]=\alpha_2,\qquad \theta[1]=\alpha_3$$

At infinity DTM is not possible. So, Pade approximation will be applied to find the value of coefficients α_1,α_2 and α_3 as a result the Pade coefficients $\alpha_1=1.0622,\alpha_2=0.8829$ and $\alpha_3=1.0968$ are substituted into the Equations (16)-(18), therefore, the expressions of $f(\eta),g(\eta)$ and $\theta(\eta)$ can be obtained in case of $A=0.5,P_r=0.7,E_c=0.3,\beta=0.5,K_p=0.6,\eta=0.5$ as

$$f(\eta)=\eta+(1.0622)\eta^2+(0.058808369)\eta^3+(0.048868576)\eta^4+(0.0066098416)\eta^5+(-0.000777637)\eta^6$$
$$+(2.736432833\times10^{-5})\eta^7+(-5.72840515\times10^{-7})\eta^8+(9.658758198\times10^{-6})\eta^9+(1.668557365\times10^{-6})\eta^{10}$$

$$g(\eta)=(-1.0622)+(0.8829)\eta+(-0.3319375)\eta^2+(0.02224225)\eta^3+(0.052165822)\eta^4+(0.015441056)\eta^5$$
$$+(0.000896317)\eta^6+(-0.00209553)\eta^7+(-0.00067914)\eta^8+(2.346214495\times10^{-5})\eta^9$$

$$\theta(\eta)=1+(1.0968)\eta+(-0.694319286)\eta^2+(-0.147186043)\eta^3+(0.000437754)\eta^4+(0.021277355)\eta^5$$
$$+(0.002001387)\eta^6+(-0.001240946)\eta^7+(-0.000591599)\eta^8+(-2.45132473\times10^{-5})\eta^9$$

5 Discussion and outcomes

Fig. 1 displays the fluid velocity variation for distinct outcomes of Micropolar parameters i.e. $A = 0.5, 1.0, 1.5, 2.0$ with the values $E_c = 0.3$,$n = 0.5$, $\beta = 0.5$, $K_p = 0.6$, $M = 0.1$, $P_r = 0.7$, $R = 1.0$. We found that outcome of the micropolar parameter increases, while fluid velocity increases rapidly.

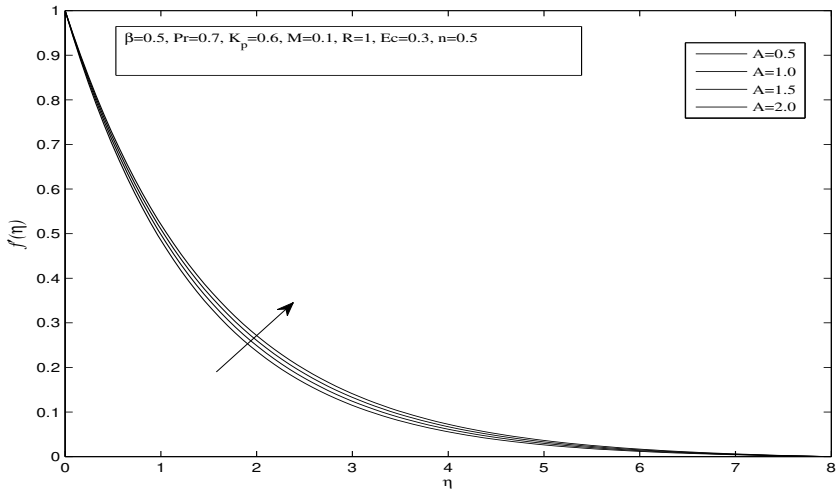

Fig. 1: Influence of micropolar parameter.

As shown in Fig. 2, the fluid velocity falls with increasing Casson parameter values from $\beta = 0.5$ to $\beta = 2.0$. The values of $A, K_p, P_r, M, n, R, E_c$ are taken as $0.5, 0.6, 0.7, 0.1, 0.5, 1.0, 0.3$ and 0.5 respectively.

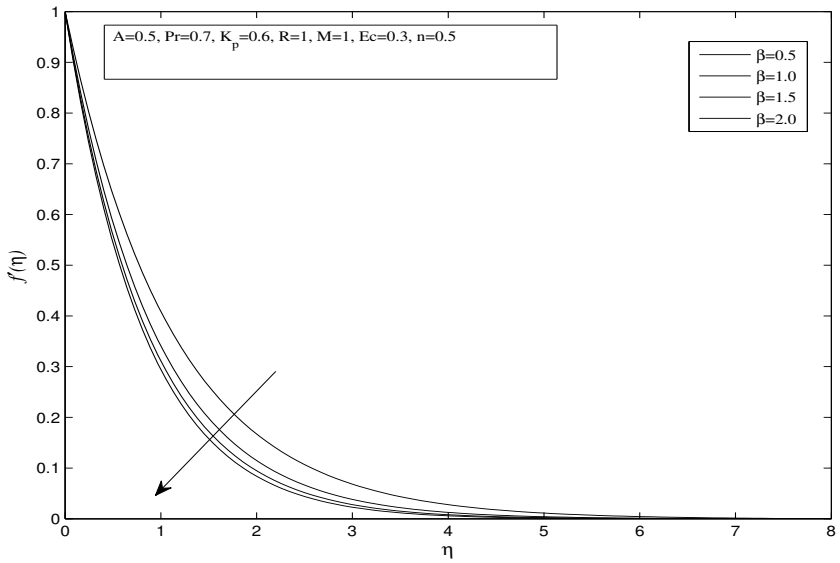

Fig. 2: Velocity Profile for Different Casson Parameters.

Fig. 3 determines the effect of fluid velocity for different values of magnetic parameters where $M = 0.1, 1.0, 3.0, 4.0$ with the values $A = 0.5, K_p = 0.6, P_r = 0.7, \beta = 0.5, n = 0.5, R = 1.0, E_c = 0.3$ and it has been noticed that a rise in the magnetic parameter leads to a drop in fluid velocity, that is, on increasing magnetic field the fluid settled down near the sheet.

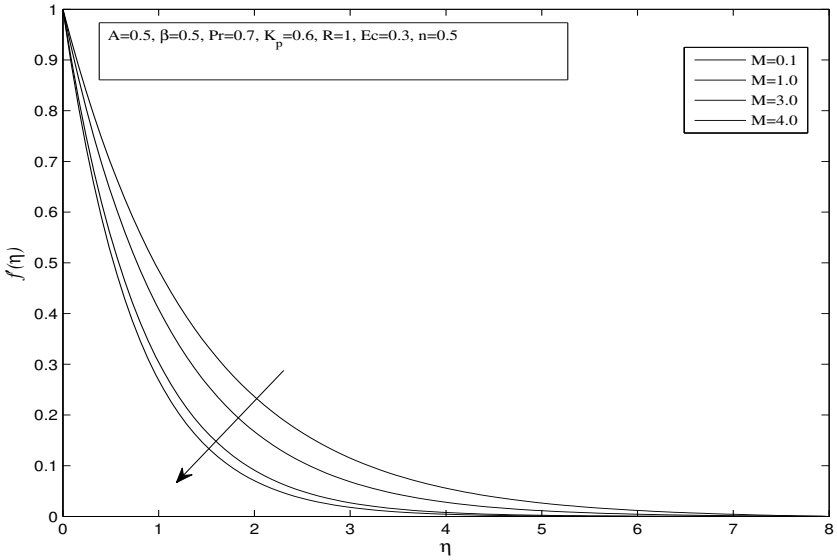

Fig. 3: Velocity Profile for distinct magnetic parameters.

In Fig. 4, we see how fluid velocity affects for distinct porosity parameters where $K_p = 0.2, 0.5, 0.7, 0.9$ with the values $A = 0.5, M = 1, P_r = 0.7, \beta = 0.5, n = 0.5, R = 1.0, E_c = 0.3$ which predicts that when the porosity parameter increases, the velocity profile reduces, that is, in the existence of porous media the fluid seem to settle down near the sheet.

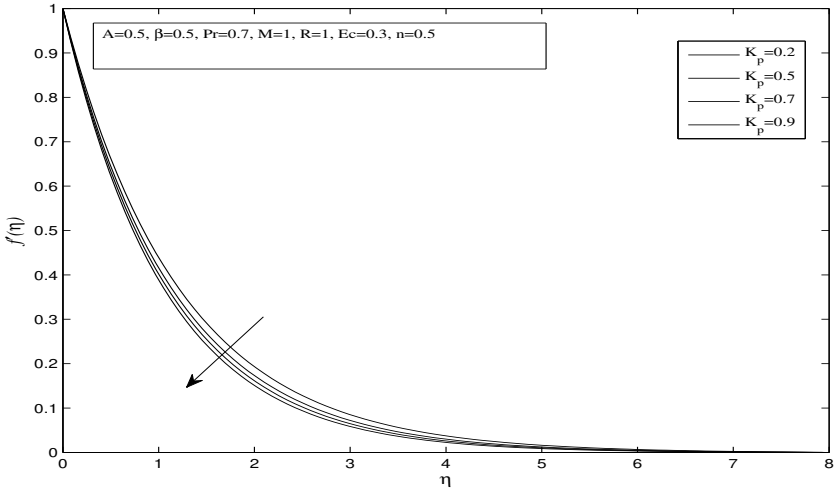

Fig. 4: Velocity Profile for distinct Porosity Parameters.

Fig. 5 elaborates the microrotation for distinct values of micropolar parameters i.e. $A = 0.5, 1.0, 1.5, 2.0$ with the values $\beta = 0.5, K_p = 0.6, M = 0.1, E_c = 0.3 n = 0.5, P_r = 0.7, R = 1.0$, and it is observed that the microrotation near the sheet rises as the micropolar parameter increases but it settles down away to sheet.

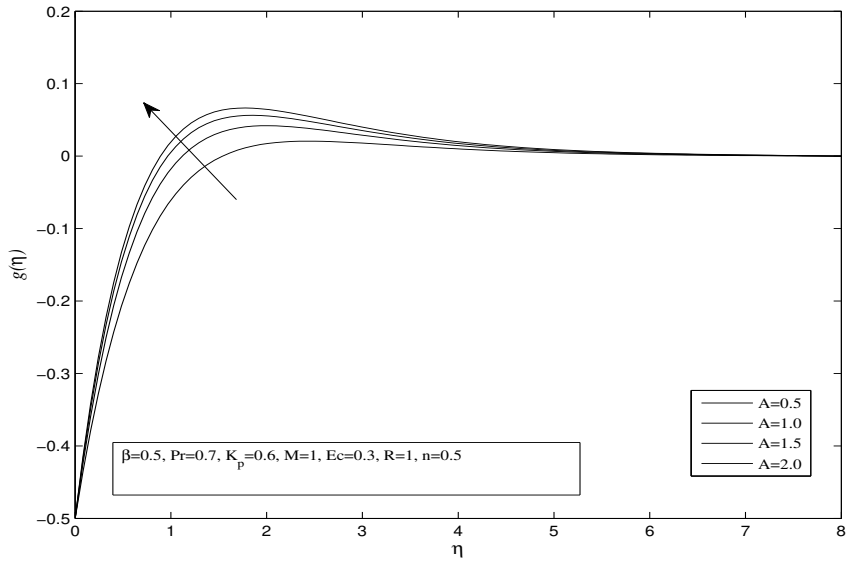

Fig. 5: Microrotation for distinct micropolar parameters.

Fig. 6 shows the microrotation for distinct Casson parameter values i.e. $\beta = 0.5, 1.0, 1.5, 2.0$ with the values $A = 0.5, K_p = 0.6, R = 1.0, M = 0.1, n = 0.5, P_r = 0.7, E_c = 0.3$ and it is noticed that the microrotation diminishes as the Casson parameter rises, that is, microelements settle down away the sheet.

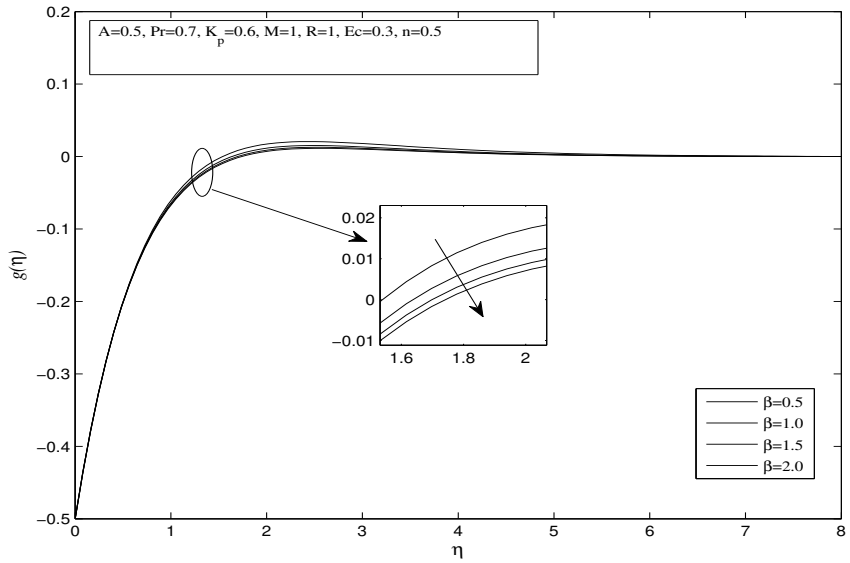

Fig. 6: Microrotation for distinct Casson parameters.

Fig. 7 demonstrates the effect of microrotation for different values of magnetic parameters $M = 1.0, 3.0, 5.0, 10.0$ with the values $A = 0.5, K_p = 0.6, P_r = 0.7, \beta = 0.5, n = 0.5, R = 1.0, E_c = 0.3$ and it is examined that as the magnetic parameter rises, the microrotation decreases, that is, as magnetic field increases the microelements start decreasing near the sheet and become settled down away the sheet.

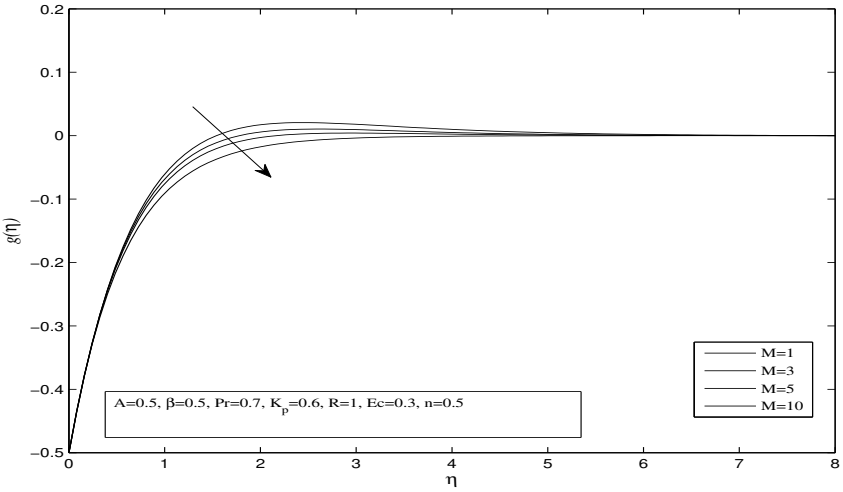

Fig. 7: Microrotation for distinct magnetic parameters.

Fig. 8 shows the effect of microrotation for distinct values of porosity parameters where $K_p = 0.1, 0.3, 0.5, 0.7$ with the values $A = 0.5, M = 1, P_r = 0.7, \beta = 0.5, n = 0.5, R = 1.0, E_c = 0.3$ and it is noticed that as the porosity parameter increases, the microrotation decreases, that is, the presence of porous medium reflects the nature of microelements which first start decreasing in rotation near the sheet and settled down away the sheet.

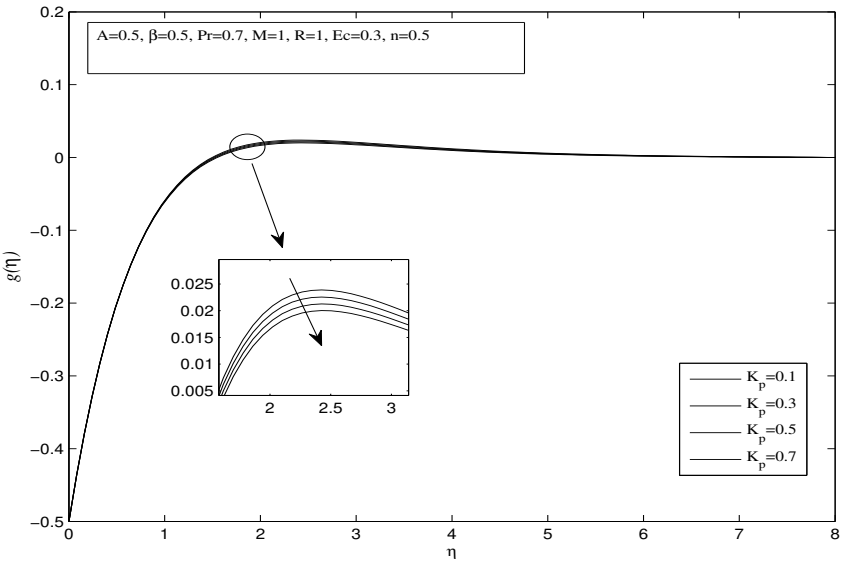

Fig. 8: Microrotation for distinct porosity parameters.

Fig. 9 shows the impact of temperature distributions for various values of Prandtl number where $P_r = 0.5, 0.6, 0.7, 1.0$ with the values $A = 0.5, M = 1.0, \beta = 0.5, , E_c = 0.3 n = 0.5, R = 1.0, K_p = 0.5$ and it has been analyzed that the temperature distribution falls as Prandtl number rises, that is, the Prandtl number has a destabilizing effect on temperature distributions.

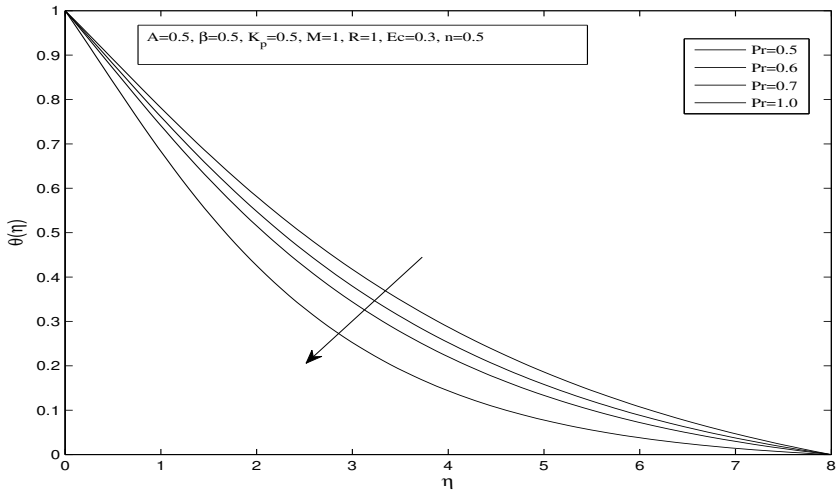

Fig. 9: Temperature distributions for distinct Prandtl numbers.

Fig. 10 determines the impact of temperature distributions for distinct values of Eckert number where $E_c = 0.2, 0.6, 1.0, 1.5$, with the values $A = 0.5, M = 1.0, K_p = 0.5, \beta = 0.5, n = 0.5, P_r = 0.7, R = 1.0$ and it has been observed that the as Eckert number increases the temperature distribution increases. That is, Eckert number has stabilizing effect on temperature.

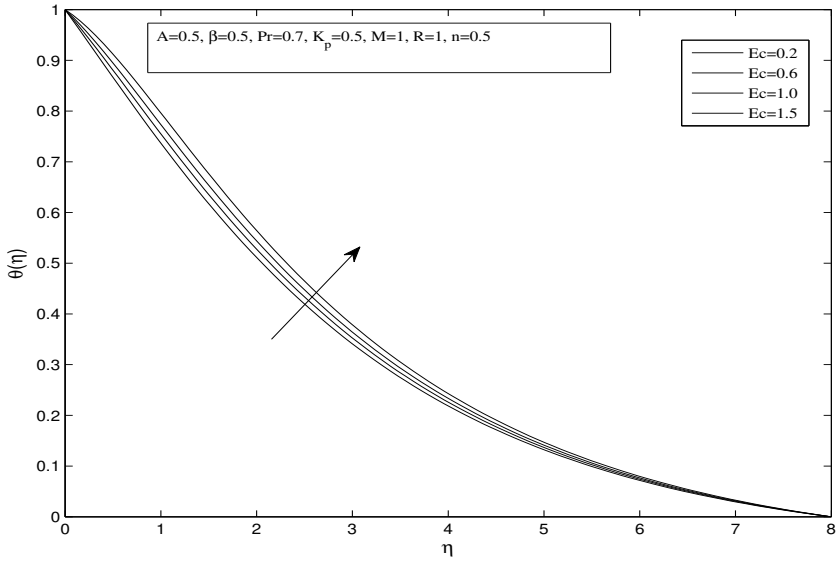

Fig. 10: Temperature distribution for distinct Eckert numbers.

6 Conclusion

The effects of several physical parameters such as the micropolar, the porosity, the Casson, and the magnetic parameters on the velocity profile, microrotation, and temperature distribution are as follows:

–The micropolar parameter enhances fluid velocity.
–The velocity of the fluid diminishes on increasing Casson fluid parameter.
–The presence of magnetic field with porous medium retards the fluid velocity.
–As micropolar parameter increases the microrotation also increases near the sheet but it settles down away to sheet.
–As Casson parameter increases the microrotation decreases, that is, microelements settle down away the sheet.
–As magnetic field increases the microelements start decreasing near the sheet and become settled down away from the sheet.
–The presence of porous medium reflects the nature of microelements which first start decreasing in rotation near the sheet and settle down away from the sheet.
–Prandtl number has a destabilizing effect on temperature distributions.
–Thermal radiation has a stabilizing effect on temperature.
–Eckert numbers have a stabilizing effect on temperature.

Acknowledgement

This research is being supported through funding from Prince Sattam bin Abdulaziz University project number (PSAU/2024/R/1445).

References

[1] Eringen, A.C., Simple micropolar fluid, Int. J. Engg. Sci., 2, 205-217 (1964).
[2] Eringen, A.C., Theory of micropolar fluids, J. Math. Mech., 16, 1-18 (1966).
[3] Wilson, A.J., Basic flows of micropolar fluids, Appl. Sci. Res., 20, 338-355 (1969).
[4] Kilne, K.A., A spin vorticity relation for unidirectional plane flows of micropolar fluids, Int. J. Engg. Sci., 15, 131-134 (1977).
[5] Gorla, R.S.R. and Takhar, H. S., Free convection boundary layer flow of a micropolar fluid past a cylinder bodies , Int. J. Engg. Sci., 25, 949-962 (1987).
[6] Adnan Y., Mixed convection in micropolar fluid flow over a horizontal plate with surface mass transfer, Int. J. Engg. Sci., 27, 1593-1602 (1989).
[7] Crane LJ. Flow past a stretching plate. Z Angew Math Phys 1970;21:645–647.
[8] T. Ariman, M.A. Turk, N.D. Sylvester, Microcontinuum fluid mechanics-a review, Int. J. Eng. Sci. 11, 905–930,. (1973)
[9] J. Prathap Kumar, J.C. Umavathi, Ali J. Chamkha, I. Pop, Fully developed free convective flow of micropolar and viscous fluids in a vertical channel, Appl. Math. Model. 34, 1175–1186,. (2010)
[10] N.A. Kelson, A. Desseaux, Effect of surface condition on flow of micropolar fluid driven by a porous stretching sheet, Int. J. Eng. Sci. 39, 1881–1897, (2001)
[11] D. Srinivasacharya, J.V. Ramana murthy, D. Venugopalam, Unsteady stokes flow of micropolar fluid between two parallel porous plates, Int. J. Eng. Sci. 39, 1557–1563, (2001)
[12] R. Bhargava, L. Kumar, H.S. Takhar, Finite element solution of mixed convection microploar fluid driven by a porous stretching sheet, Int. J. Eng. Sci. 41, 2161–2178. (2003)
[13] F.S. Ibrahim, A.M. Elaiw, A.A. Bakr, Influence of viscous dissipation and radiation on unsteady MHD mixed convection flow of micropolar fluids, Appl. Math. Inf. Sci. 2, 143–162, (2008)
[14] M.E. Ali, E. Magyari, Unsteady fluid and heat flow induced by a submerged stretching surface while its steady motion is slowed down gradually, Int. J. Heat Mass Transf. 50, 188–195, (2007).
[15] S. Mukhopadhyay, Effect of thermal radiation on unsteady mixed convection flow and heat transfer over a porous stretching surface in porous medium, Int. J. Heat Mass Transf. 52, 3261–3265,.(2009)
[16] N.A. Yacos, A. Ishak, I. Pop, Melting heat transfer in boundary layer stagnation-point flow towards a stretching/shrinking sheet in a micropolar fluid, Computers and Fluids, 47, 16–21, 2011
[17] H. Rosali, A. Ishak, I. Pop, Micropolar fluid flow towards a stretching/shrinking sheet in a porous medium with suction, Int. Commu. Heat Mass Transfer. 39, 826–829, (2012).
[18] D. Bhukta, G.C. Dash, S.R. Mishra, Heat and mass transfer on MHD flow of a viscoelastic fluid through porous media over a shrinking sheet, Int. Scholarly Res. Notices, 14, 1–11, (2024) Article ID 572162.
[19] M.A.A. Mahmood, S.E. Waheed, MHD flow and heat transfer of a micropolar fluid over a stretching surface with heat generation (absorption) and slip velocity, J. Egypt Math. Soc. 20(1) 20–27, (2012).

[20] Ahmad, S., et al., Effects of Thermal Radiation on MHD Axisymmetric Stagnation Point Flow and Heat Transfer of a Micropolar Fluid over a Shrinking Sheet, World Applied Sciences Journal, 15, 835-848, (2011)
[21] Eldabe, N. T., Abou-Zeid, M. Y., Magnetohydrodynamic Peristaltic Flow with Heat and Mass Transfer of Micropolar Biviscosity Fluid through a Porous Medium between Two Co-Axial Tubes, Arab Journal Science Engineering, 39, 5045-5062, (2014)
[22] El-Dabe, N. T. M., et al., Heat and Mass Transfer of Magnetohydrodynamic Pulsatile Flow of Casson Fluid with Couple Stress through Porous Medium, International Journal of Current Engineering and Technology, 6, 1414-1421, (2016)
[23] Mekheimer, K. S., Non-Linear Peristaltic Transport through a Porous Medium in an Inclined Planar Chan- nel, Journal of Porous Media, 6, 190-202, (2003)
[24] Zueco, J., Ahmed, S., Combined Heat and Mass Transfer by Mixed Convection MHD Flow Along a Po- rous Plate with Chemical Reaction in Presence of Heat Source, Applied Mathematics and Mechanics, 31, 1217-1230, (2010)
[25] Mehmood, Z., et al., Numerical Investigation of Micropolar Casson Fluid over a Stretching Sheet with Internal Heating, Communication Theory of Physics, 67, 443-448, (2017)
[26] Iqbal, Z., et al., Impact of Inclined Magnetic Field on Micropolar Casson Fluid Using Keller Box Algorithm, The European Physical Journal Plus, 15, 132-175, (2017)
[27] Sepasgozar, S., Faraji, M., & Valipour, P., Application of differential transformation method (DTM) for heat and mass transfer in a porous channel, Propulsion and Power Research, 6, 41–48 (2017).